Journal of Computations & Modelling, vol.3, no.1, 2013, 1-31
ISSN: 1792-7625 (print), 1792-8850 (online)
Scienpress Ltd, 2013

Theoretical study on the behaviour of rectangular concrete beams reinforced internally with GFRP reinforcements under pure torsion

A. Prabaghar[1] and G. Kumaran[2]

Abstract

Theoretical Modelling of rectangular concrete beams reinforced internally with Glass Fibre Reinforced Polymer (GFRP) reinforcements under pure torsion is carried out in this study. Different parameters like grade of concrete, beam longitudinal reinforcement ratio and transverse stirrups spacing are considered. The basic strength properties of concrete, steel and GFRP reinforcements are determined experimentally. Theoretical torque verses twist relationship is established for various values of torque and twist using elastic, plastic theories of torsion. Finally the ultimate torque is determined using space truss analogy and softening truss model for different parameters and based on this study, a good agreement is made between the theoretical behaviour GFRP reinforced and conventionally reinforced beams.

Keywords: pure torsion, beam, GFRP reinforcements, steel, theoretical model

[1] Annamalai University, India, e-mail: aprabaghar@yahoo.co.in
[2] Annamalai University, India, e-mail: ganapathykumaran@rediffmail.com

Article Info: *Received* : December 22, 2012. *Revised* : January 29, 2013
Published online : March 31, 2013

1 Introduction

Fibre Reinforced Polymer (FRP) materials are becoming a new age material for concrete structures. Its use has been recommended in ACI codes. But in India its applicability is rare in view of the few manufacturers and lacking in commercial viability. The advantages of the FRP materials lie in their better structural performance especially in aggressive environmental conditions in terms of strength and durability (Machida 1993; ACI 440R-96 1996; Nanni 1993). FRP materials are commercially available in the form of cables, sheets, plates etc. But in the recent times FRPs are available in the form of bars which are manufactured by pultrusion process which are used as internal reinforcements as an alternate to the conventional steel reinforcements. These FRP bars are manufactured with different surface imperfections to develop good bond between the bar and the surrounding concrete. Fibre reinforcements are well recognised as a vital constituent of the modern concrete structures. FRP reinforcements are now being used in increasing numbers all over the world, including India. FRP reinforcements are preferred by structural designers for the construction of seawalls, industrial roof decks, base pads for electrical and reactor equipment and concrete floor slabs in aggressive chemical environments owing to their durable properties.

Due to the advantages of FRP reinforcements in mind, many research works have been carried out throughout the world on the use of FRP reinforcing bars in the structural concrete flexural elements like slabs, beams, etc. (Nawy *et al* 1997; Faza and GangaRao 1992; Benmokrane 1995; Sivagamasundari 2008; Deiveegan *et al* 2011; Saravanan *et al* 2011). Therefore the present study discusses mainly on the behaviour of beams reinforced internally with GFRP reinforcements under pure torsion. The scope of the present study is restricted to with the GFRP reinforcements because of their availability in India. First part of this study covers the theoretical analysis based on the existing using space truss formulation for conventionally reinforced and GFRP reinforced beams. Second

part of this study is related to the theoretical formulation using softened truss model for steel and GFRP reinforced beams. Finally, the results are summarised based on the theoretical analysis and with the existing theories.

2 Materials

2.1 Concrete

Normal Strength Concrete (NSC) of grades M20 and M30 are used in this study. Ordinary Portland Cement is used to prepare the concrete. The maximum size of aggregate used is 20 mm and the size of fine aggregate ranges between 0 and 4.75 mm. After casting, the specimens are allowed to cure in real environmental conditions for about 28 days so as to attain strength. The test specimens are generally tested after a curing period of 28 days.

Table 1: Properties of Concrete

Description	**M 20 grade** (m_1)	**M 30 grade** (m_2)
Ratio	1:1.75:3.75	1:1.45:2.85
W/C Ratio	0.53	0.45
Average Compressive Strength of cubes	32.25 MPa	44.14 MPa

The strength of concrete under uni-axial compression is determined by loading ‘standard test cubes’ (150 mm size) to failure in a compression testing machine, as per IS 516 - 1959. The modulus of elasticity of concrete is determined by loading ‘standard cylinders’ (150 mm diameter and 200 mm long) to failure in a compression testing machine, as per IS 516: 1959. The mix proportions of the

NSC are carried out as per Indian Standards (IS) 10262-1982 and the average compressive strengths are obtained from laboratory tests (Sivagamasundari 2008; Deiveegan *et al* 2011; Saravanan *et al* 2011) and are depicted in Table 1.

2.2 Reinforcements

The mechanical properties of all the types of GFRP reinforcements as per ASTM-D 3916-84 Standards and steel specimens as per Indian standards are obtained from laboratory tests and the results are tabulated in Table 2. The tensile strength of steel reinforcements (*S*) used in this study, conforming to Indian standards and having an average value of the yield strength of steel is considered for this study. GFRP reinforcements used in this study are manufactured by pultrusion process with the E-glass fibre volume approximately 60% and these fibres are reinforced with epoxy resins. Previous studies were carried out with three different types of GFRP reinforcements (grooved, sand sprinkled & threaded) (ACI 440R-96; Sivagamasundari 2008; Deiveegan *et al* 2011; Saravanan *et al* 2011) with different surface indentations and are designated as F_g, F_s *and* F_t. In this study threaded type GFRP reinforcement is used in place of conventional steel. The diameters of the longitudinal and transverse reinforcements are 12 mm and 8 mm respectively. The standard minimum diameters of the reinforcements as per Indian standards are adopted in this study.

The tensile strength properties are ascertained as per ACI standards shown in Table 1(b) and are validated by conducting the tensile tests at SERC, Chennai. The GFRP reinforcements are provided with end grips to avoid the crushing of ends. The typical failure pattern of the GFRP reinforcement is shown in Figure 1. The stress-strain curve of the reinforcements used in the study are obtained from the experimental study is shown clearly in Figure 2. The compressive modulus of elasticity of GFRP reinforcing bars is smaller than its tensile modulus of elasticity (ACI 440R-96; Lawrence C. Bank 2006; Sivagamasundari 2008). It varies

between 36-47 GPa which is approximately 70% of the tensile modulus for GFRP reinforcements. Under compression GFRP reinforcements have shown a premature failures resulting from end brooming and internal fibre micro-buckling.

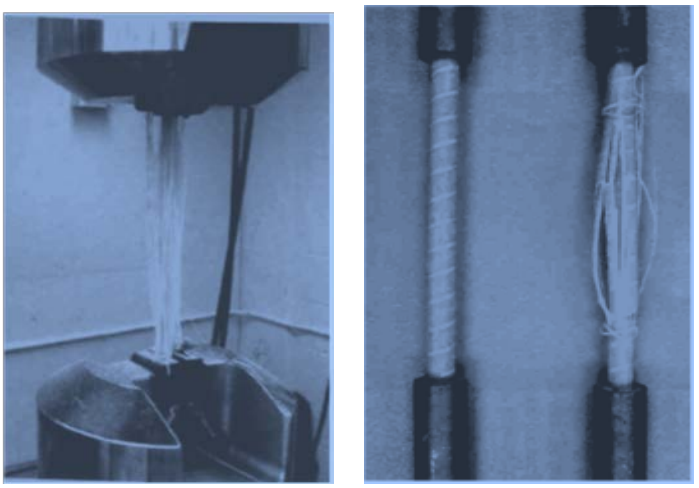

Figure 1: Failure of GFRP reinforcements during tensile test

In this study, GFRP stirrups are manufactured by Vacuum Assisted Resin Transfer Moulding process, using glass fibres reinforced with epoxy resin (ACI 440R-96; Sivagamasundari *et al* 2008; Deiveegan *et al* 2011; Saravanan *et al* 2011). Based on the experimental study, it is observed that the strength of GFRP stirrups at the bend location (bend strength) is as low as 50% of the strength parallel to the fibres. However, the stirrup strength in straight portion is comparable to the yield strength of conventional steel stirrups. Therefore, in this study, GFRP stirrups strength is taken as 30% of its tensile strength ie. 150 MPa.

Table 2: Properties of reinforcements

Properties	Threaded GFRP (F_t)	Steel Fe 415 (S)
Tensile strength (MPa)	525	475
Longitudinal modulus (GPa)	63.75	200
Strain	0.012	0.002
Poisson's ratio	0.22	0.3

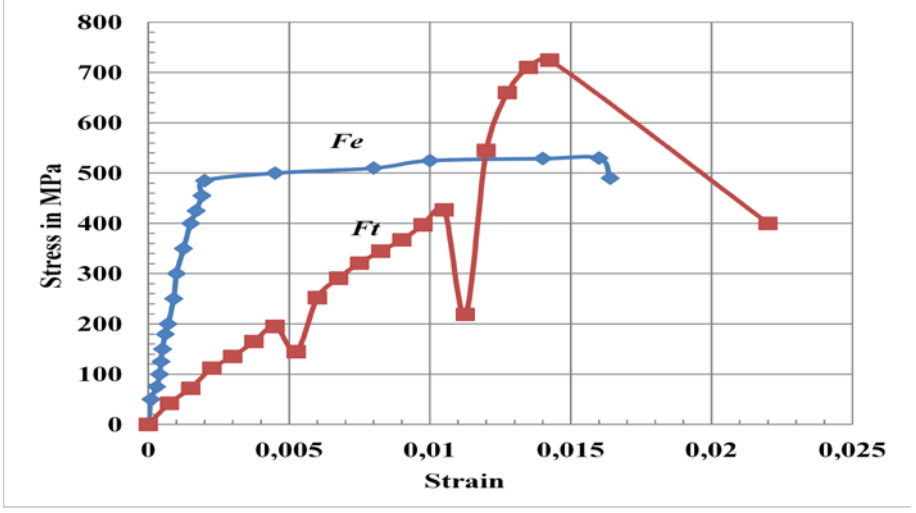

Figure 2: Stress-Strain curve for all the reinforcements involved in the present study

3 Theoretical Investigation

Theoretical torque verses twist relationship is established for various values of torque and twist using elastic, plastic theories of torsion and also the ultimate torque is determined using space truss analogy (Hsu 1968; MacGregor *et al* 1995; Rasmussen *et al* 1995; Asghar *et al* 1996; Khaldown *et al* 1996; Liang *et al* 2000; Luis *et al* 2008; Chyuan 2010). The theoretical investigation consists different

rectangular beams and are designated are as follows; $Bp_1m_1F_e\ s_1$; $Bp_1m_1F_t\ s_1$; $Bp_1m_2F_e\ s_1$; $Bp_1m_2F_t\ s_1$; $Bp_2m_1F_e\ s_1$; $Bp_2m_1F_t\ s_1$; $Bp_2m_2F_e\ s_1$; $Bp_2m_2F_t\ s_1$, $Bp_1m_1F_e\ s_1$; $Bp_1m_1F_t\ s_1$; $Bp_1m_2F_e\ s_1$; $Bp_1m_2F_t\ s_1$; $Bp_2m_1F_e\ s_1$; $Bp_2m_1F_t\ s_1$; $Bp_2m_2F_e\ s_1$; $Bp_2m_2F_t\ s_2$. These beams are reinforced internally with threaded type Glass Fibre Reinforced Polymer Reinforcements and conventional steel reinforcements with different grades of concrete and steel reinforcement ratio under pure torsion is considered in this study. The entire concrete beam is supported on saddle supports which can allow rotation in the direction of application of torsion as shown in Figure 3.

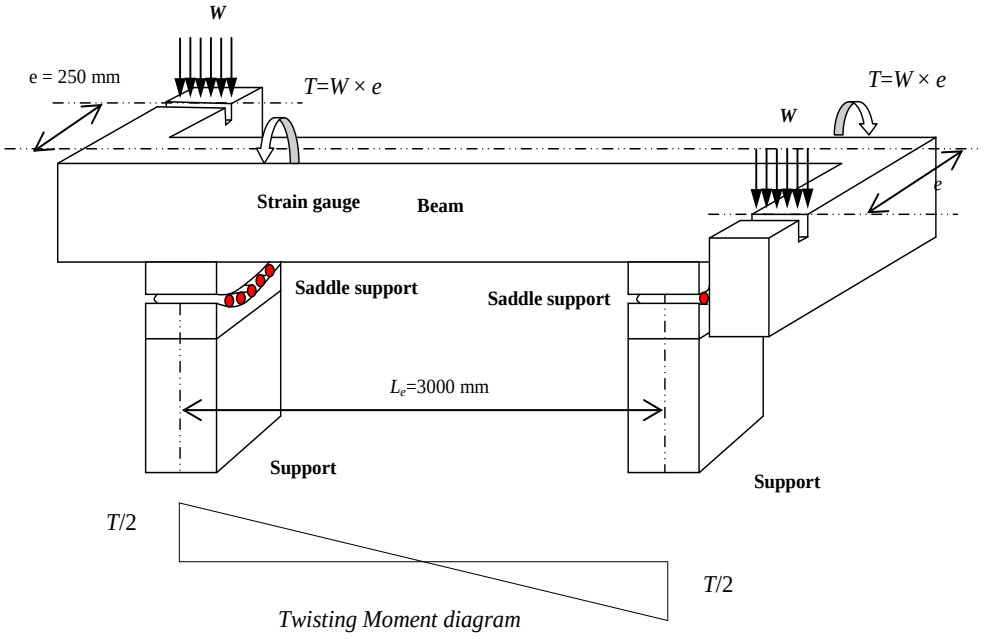

Figure 3: Beam supported on saddle support

Parameters considered for analyzing the GFRP /steel reinforced concrete beams are as follows:

B = 160 mm; D = 275 mm; b_1 = 118 mm; d_1 = 233 mm; E_{GFRP} = 63750 N/mm^2;

m_1 = 32.25 MPa; m_2 = 44.14 MPa; E_{c1}= $5000\sqrt{f_{ck}}$ = $5000\sqrt{32.25}$ = 29395 N/mm^2; E_{c1}= $5000\sqrt{f_{ck}}$ = $5000\sqrt{44.14}$ = 33219 N/mm^2; Al = 113×6= 678.24 mm^2; A_t = 2× 50.3 = 100.6 mm^2; f_{GFRP} =525 MPa; $f_{GFRP\text{-}S}$ =150 MPa; S_1 = 75 mm; S_2 = 50 mm. In the figures the curves to be read as,Exp - Experimental curve; Th-space = Theoretical- space truss analogy and Th-soft = Theoretical- softened truss model. Table 3 shows the various parameters involved in the present study.

Table 3: Various Parameters involved

Parameters	Description	Designation
Types of reinforcements	Threaded GFRP	*Ft*
	Conventional	*Fe*
Concrete grade	Two grades of concrete	m_1 & m_2
Beam size	160 x 275 mm	*B*
Reinforcement ratios	1. 0.56% (2-12 mm bars top & Bottom) 2. 0.85% (3-12 mm bars top & Bottom)	p_1 & p_2
Spacing of stirrups	75 mm & 50 mm	S_1 & S_2

3.1 Space Truss Analogy

The general theoretical torque twist curve T–θ curves are plotted for three stages and are defined by their (θ;T) coordinates (Hsu 1968; Collins 1973). These coordinates are shown in Figure 4.

Stage 1 represents the beam's behaviour before cracking. The slope of the curve represents the elastic St. Venant stiffness $(GC)^I$). In this stage the curve can be assumed as a straight line with origin in the point (0;0) and end in (θ_{el};T_{el}). The theoretical model considered in this study for this stage is based on Theory of Elasticity.

After cracking, the beams suffers a sudden increase of twist after what it resets the linear behaviour. This stage is identified as Stage 2. It starts at (θ_{cr};T_{cr}) and ends at a certain level of twist (θ_{cr}). The slope of stage-2 represents the torsional stiffness in cracked stage $(GC)^{II}$. The model considered for stage-2 is based on the space truss analogy with 45° inclined concrete struts and linear behaviour for the materials. The points of the T–θ curve from which, the nonlinear behaviour is defined by means of two different criteria. The first one corresponds to finding the point for which at least one of the torsion reinforcements (longitudinal or transversal) reaches the yielding point. The second criterion corresponds to finding the point for which the concrete struts starts to behave nonlinearly, due to high levels of loading (this situation may occur before any reinforcement bar yields).

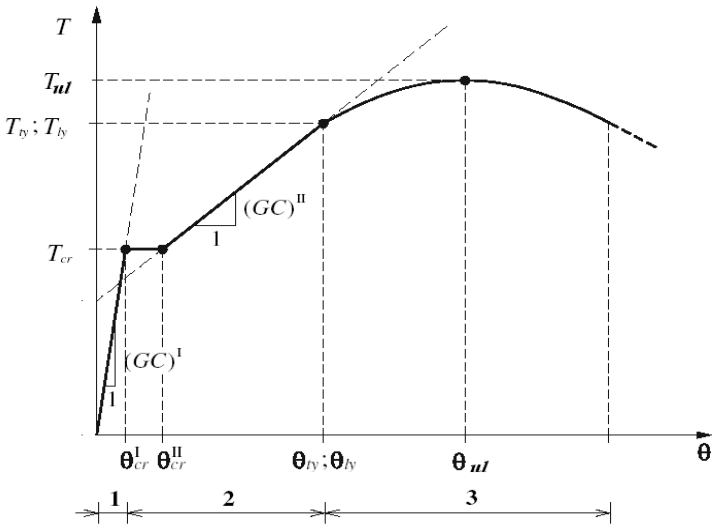

Figure: 4 Typical T-θ curve for a reinforced concrete beam under pure torsion

where, T_{cr} = Cracking torque; θ_{cr} = Twist corresponding to T_{cr} for the stage 1 (limit for linear elastic analysis in non cracked and cracked stage); T_{ly} = Torque corresponding to yielding of longitudinal reinforcement; θ_{ly} = Twist

corresponding to T_{ly}; T_{ty} = Torque corresponding to yielding of transversal reinforcement; θ_{ty} = Twist corresponding to T_{ty}; T_{ul} = Ultimate (maximum) torque; θ_{ul} = Maximum twist at beam's failure. $(GC)^{I}$ = Torsional stiffness of Zone 1 (for linear elastic analysis in non cracked stage); $(GC)^{II}$ = Torsional stiffness of Zone 2 (for linear elastic analysis in cracked stage). The linear elastic torque is clearly depicted in Figure 5.

Stage 3 of the curve was plotted with non linear behaviour of the materials and considering the Softening Effect. In this study, space truss analogy is used to the locate the following coordinates (θ_{ty};T_{ty}) & (θ_{ul};T_{ul}). The space truss model with softening effect is not considered since it involves iterative procedure. The three stages are identified in the T–θ curve of Figure 4 are characterized separately.

Stage: 1 Linear Elastic Torque (T_{el}, θ_{el}):

For rectangular sections using St. Venant theory, the maximum torsional shear stress occurs at the middle of the wider face (Hsu 1968), and has a value given by

$$\tau_{t,\max} = \frac{T}{\alpha b^2 D} \tag{1}$$

where T is the twisting moment (torque), b (160 mm) and D (275 mm) are the cross-sectional dimensions (b being smaller), and α is a St. Venant coefficient whose value depends on the D/b ratio; α lies in the range 0.21 to 0.29 for D/b varying from 1.0 to 5.0 respectively. Therefore α=0.2243; $\tau_{t,\max}$ (MPa units) of about $0.2\sqrt{f_{ck}}$

Elastic torque is given by

$$T_{el} = \alpha b^2 D \times \tau_{t,\max} \tag{2}$$

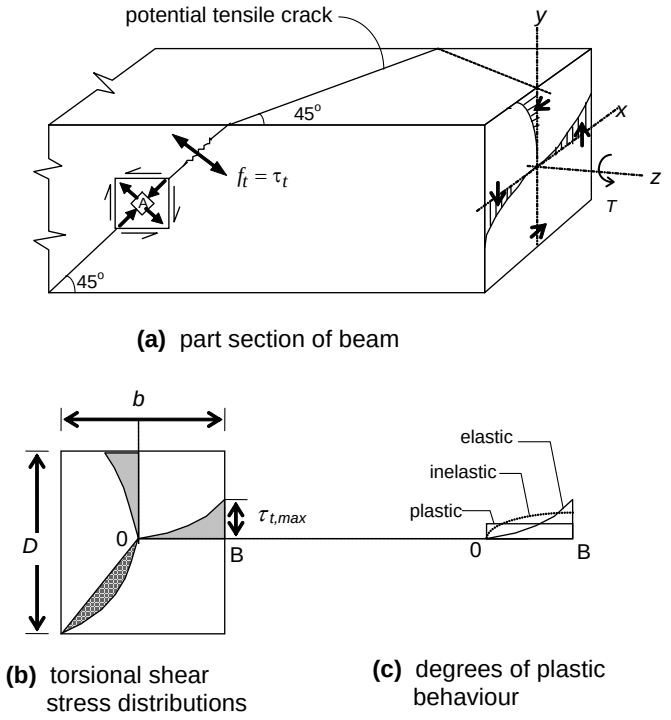

Figure 5: Torsional shear stresses in a rectangular beam

Using Torque-Twist relationship based on linear elastic analysis is given by

$$\frac{T_{el}}{C} = \frac{G \times \theta_{el}}{l} \tag{3}$$

From the above, the twist θ_{el} per unit length of a beam can be expressed as

$$\theta_{el} = \frac{T_{el} \times l}{G \times C} \tag{4}$$

where T_{el} is the elastic torque, *GC* is the Torsional Rigidity, obtained as a product of the Shear Modulus, *G* and the geometrical parameter *C* of the section. Since *G* is equal to $E_C/[2(1 + \gamma)]$, where E_C is the Young Modulus of concrete and γ is the Poisson Coefficient, and γ = 0.25. Therefore G=0.4 E_C. The stiffness factor *C* (for a plain rectangular section of size $b \times D$, with $b < D$), based on 'St.Venant theory is given by the following expression

$$C = \beta b^3 D \tag{5}$$

where β is a constant which may be calculated,

$$\beta = \left(1 - 0.63\frac{b}{D}\right)\Big/3 = \quad \beta = \left(1 - 0.63 \times \frac{160}{275}\right)\Big/3 = 0.211$$

Stage: 2 First crack Torque (T_{cr1}, θ_{cr1}): (Linear Elastic Analysis in cracked phase)

The strength of a torsionally reinforced member at torsional cracking T_{cr} is practically the same as the failure strength of a plain concrete member under pure torsion. Although several methods have been developed to compute T_{cr} , the *plastic theory* approach based on Indian standards is described here. The cracking Torque is given by,

$$\Rightarrow T_{cr} = \tau_{t,\max}\frac{b^2}{2}\left(D - b/3\right) \tag{6}$$

Studies show that the torsion reinforcement has a negligible influence on the torsional stiffness. However the presence of torsion reinforcement does delay the cracking point. Hsu, 1968 showed that the effective cracking moment, $T_{cr,\,ef}$, may be computed by:

$$\Rightarrow T_{cr,ef} = \left(1 + 4\rho_t\right)T_{cr} \tag{7}$$

Where, A_l = total area of the longitudinal reinforcement; A_t = area of one leg of the transversal reinforcement; s = spacing of stirrups; l_s = perimeter of the centre line of the stirrups.

Using Torque-Twist relationship based on linear elastic analysis is given by

$$\frac{T_{cr,eff}}{C} = \frac{G \times \theta_{cr,eff}}{l} \tag{8}$$

From the above, the twist $\theta_{el,eff}$ per unit length of a beam can be expressed by,

$$\theta_{cr,eff} = \frac{T_{el,eff} \times l}{(GC)^I} \tag{9}$$

Torsional stiffness is given by,

$$(GC)^I = K_t^I = 0.4 \times 5000\sqrt{f_{cu}} \times \mathrm{C} \quad (10)$$

Stage: 3 Ultimate Torque (T_{ul}, θ_{ul}):

The use of the *thin-walled tube analogy* (or) *space truss analogy* the shear stresses are treated as constant over a finite thickness *t* around the periphery of the member, allowing the beam to be represented by an equivalent hollow beam of uniform thickness. Within the walls of the tube, torque is resisted by the shear flow *q*, which has units of force per unit length. In the analogy, *q* is treated as a constant around the perimeter of the tube. To predict the cracking behaviour, the concrete tube may be idealized through the special truss analogy proposed by Rausch. The space truss analogy is essentially an extension of the *plane truss analogy* used to explain flexural shear resistance. The 'space-truss model' is an idealisation of the effective portion of the beam, comprising the longitudinal and transverse torsional reinforcement and the surrounding layer of concrete. It is this 'thin-walled tube' which becomes fully effective at the post-torsional cracking phase. The truss is made up of the corner longitudinal bars as stringers, the closed stirrup legs as transverse ties, and the concrete between diagonal cracks as compression diagonals. Assuming torsional cracks (under pure torsion) at 45^o to the longitudinal axis of the beam and considering equilibrium of forces normal to section AB. It is this 'thin-walled tube' which becomes fully effective at the post-torsional cracking phase. The truss is made up of the corner longitudinal bars as stringers, the closed stirrup legs as transverse ties, and the concrete between diagonal cracks as compression diagonals (Unnikrishna pillai and Devdoss Menon 2003).

$$q = \frac{T_u}{2A_0} = \frac{T_u}{2b_1 d_1} \quad (11)$$

$$A_o = b_1 d_1 \quad (12)$$

where A_o is the area enclosed by the centre line of the thickness; b_1 and d_1 denote the centre-to-centre distances between the corner bars in the directions of the

width and the depth respectively Assuming torsional cracks (under pure torsion) at 45^o to the longitudinal axis of the beam, and considering equilibrium of forces normal to section, the total force in each stirrup is given by $qs_v \ tan\ 45^o = qs_v$ where s_v is the spacing of the (vertical) stirrups. Further, assuming that the stirrup has yielded in tension at the ultimate limit state or (Design stress = $\phi\ f_y$; ϕ = partial safety factor for steel=0.87; f_y = yield strength of steel; Design stress for GFRP reinforcements = $\phi\ f_{GFRP}$; ϕ = strength reduction factor for GFRP reinforcements = 0.80; f_{GFRP} tensile strength of GFRP reinforcements); it follows from force equilibrium that

$$A_t(\phi\ f_{y/GFRP}) = qs_v \tag{13}$$

where A_t is the cross-sectional area of the stirrup (equal to $A_{sv}/2$ for two legged stirrups). Substituting eqn. 12 & 13 in eqn. 11, the following expression is obtained for the ultimate strength $T_u = T_{uR}$ in torsion:

$$T_{uR} = 2A_t b_1 d_1 (\phi\ f_{y/GFRP}) \big/ s_v \tag{14}$$

Further, assuming that the longitudinal steel (symmetrically placed with respect to the beam axis) has also yielded at the ultimate limit state, it follows from longitudinal force equilibrium that (Figure 6):

$$A_l(\phi\ f_{y/GFRP}) = \frac{q}{\tan 45^o} \times 2(b_1 + d_1) \tag{15}$$

where $A_l \equiv$ the total area of the longitudinal steel/GFRP reinforcements and f_{yl} yield strength of steel; f_{GFRP} tensile strength of GFRP reinforcements. Substituting eqn. 11 in 15, the following expression is obtained for the ultimate strength $T_u = T_{uR}$ in torsion:

$$T_{uR} = A_l b_1 d_1 (\phi\ f_{y/GFRP}) \big/ (b_1 + d_1) \tag{16}$$

The two alternative expressions for T_{uR} viz. eqn. 14 and eqn. 16, will give identical results only if the following relation between the areas of longitudinal steel and transverse steel (as torsional reinforcement) is satisfied:

$$A_l = A_{t/GFRP-t} \times \frac{2(b_1 + d_1)}{s_v} \times \frac{f_{y/GFRP-t}}{f_{y/GFRP}} \tag{17}$$

where $A_t \equiv$ cross sectional area of the 2 legged stirrups; $A_{GFRP\text{-}t} \equiv$ cross sectional area of the 2 legged GFRP stirrups; $f_{yt} \equiv$ yield strength of steel; $f_{GFRP\text{-}t} \equiv$ tensile strength of GFRP stirrups. If the relation given by the eqn. 17 is not satisfied, then T_{uR} may be computed by combining eqn. 14 and eqn. 16, taking into account the areas of both transverse and longitudinal reinforcements:

$$T_{uR} = 2b_1 d_1 \sqrt{\left(\frac{A_t f_y}{s_v}\right)\left(\frac{A_l \times f_{yl}}{2(b_1 + d_1)}\right)} \times 0.87 \tag{18}$$

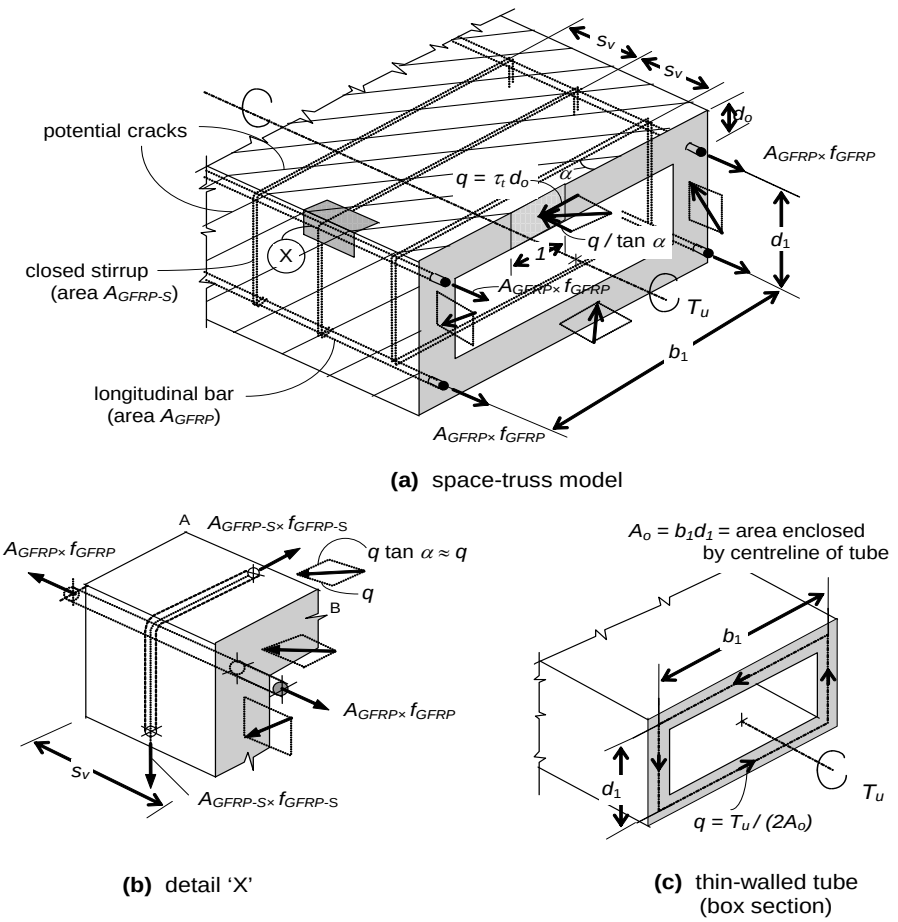

Figure 6: Space-truss model for GFRP reinforced beams

To ensure that the member does not fail suddenly in a brittle manner after the development of torsional cracks, the torsional strength of the cracked reinforced section must be at least equal to the cracking torque T_{cr} (computed without considering any safety factor). The ultimate torque T_{ul} may be computed by considering the contributions of both transverse and longitudinal reinforcements:

$$T_{ul} = 2b_1 d_1 \sqrt{\left(\frac{A_{t/GFRP} f_{y/GFRP}}{s_v}\right)\left(\frac{A_{l/GFRP} \times f_{l/GFRP}}{2(b_1 + d_1)}\right)} \times \phi \tag{19}$$

To predict the cracking behaviour, the concrete tube may be idealized through the spaces truss analogy proposed by Rausch in 1929. Based on Hsu, the following equation for the torsional stiffness $(GC)^{II}$ of rectangular sections:

$$(GC)^{II} = \frac{E_s b_1^2 d_1^2 BD}{(b_1 + d_1)^2 \left[\frac{2mBD}{(b_1 + d_1)D} + \frac{1}{\rho_l} + \frac{1}{\rho_t}\right]} \tag{20}$$

Transverse GFRP **reinforcement alone:**

Considering shear –torsion interaction with Vu=0, which corresponds to space truss formulation, considering the contribution of the transverse reinforcement alone,

$$T_{ty} = A_t b_1 d_1 (f_{GFRP-t})/s_v \tag{21}$$

The values obtained from the space truss analogy for various parameters for the conventionally reinforced and GFRP reinforced specimens are shown in Table 4.

3.2 Softened Truss Model

The softening truss model, developed by Hsu & Mo (1985), is similar to the space truss model described above, except that it utilizes the full concrete cross section and takes the softening of the concrete into consideration. The softening of

concrete is based on an assumed effective transverse compressive stress component, which is used to predict the torsional behaviour of reinforced concrete. The model was developed according to the fundamental principles of the mechanics of materials, stress equilibrium, strain compatibility, and the constitutive law of materials. In this model, the constitutive law of materials is given in terms of the stress-strain curve of the softened concrete shown in Figure 7.

The equation for the ascending portion of the stress-strain curve of normal strength concrete is modelled as:

$$f_c = f_c^{'}\left[2\left(\frac{\varepsilon_c}{\varepsilon_o}\right) - \frac{1}{\xi}\left(\frac{\varepsilon_c}{\varepsilon_o}\right)^2\right] \tag{22}$$

where $f_c \equiv$ stress in concrete corresponding to the strain ε_c; $f_c^{'} \equiv$ compressive strength of concrete; $\varepsilon_c \equiv$strain in diagonal concrete struts; $\varepsilon_o \equiv$ strain at maximum concrete compressive stress = 0.002; $\xi \equiv$ Softening coefficient

$$\xi = \frac{1}{\sqrt{\frac{\varepsilon_l+\varepsilon_s+2\varepsilon_d}{\varepsilon_d}-0.3}} \tag{23}$$

where $\varepsilon_l \equiv$ strain in longitudinal reinforcement; $\varepsilon_s \equiv$ strain in stirrups; $f_k \equiv \xi f_c^{'}$ peak softened compressive strength; $\varepsilon_k \equiv \xi\varepsilon_o$ - softened strain corresponding to peak softened compressive strength.

The equation of the descending portion of the stress-strain curve is given as:

$$f_c = f_k\left[1 - \left(\frac{\varepsilon_c-\varepsilon_k}{2\varepsilon_o-\varepsilon_k}\right)^2\right] \tag{24}$$

The torque is obtained from equilibrium equations. The detailed derivation of the equations and the solution technique for the ultimate torsional capacity can be found elsewhere (Hsu & Mo 1985; Hsu 1988).

Table 4: Results of space truss analogy for various parametric conditions

Specimens	T_{el}	θ_{el}	T_{cr1}	θ_{cr1}	T_{eff}	θ_{eff}	T_{yt}	θ_{yt}	T_{ul}	θ_{ul}
$Bp_1m_1F_eS_1$	1.79	0.051	3.22	0.092	3.61	0.103	12.27	3.29	20.49	5.51
$Bp_1m_1F_t\,S_1$	1.79	0.051	3.22	0.092	3.61	0.103	3.56	3.08	12.11	10.45
$Bp_1m_2F_e\,S_1$	2.09	0.051	3.77	0.092	4.2	0.103	12.27	3.27	20.5	5.51
$Bp_1m_2F_t\,S_1$	2.09	0.051	3.77	0.092	4.2	0.103	3.56	3.1	14.83	12.81
$Bp_2m_1F_e\,S_1$	1.79	0.051	3.22	0.092	3.67	0.105	12.27	3.29	25.12	6.74
$Bp_2m_1F_t\,S_1$	1.79	0.051	3.22	0.092	3.67	0.105	5.18	5.02	14.82	12.82
$Bp_2m_2F_e\,S_1$	2.09	0.051	3.77	0.092	4.29	0.105	12.67	3.27	25.1	6.70
$Bp_2m_2F_t\,S_1$	2.09	0.051	3.77	0.092	4.29	0.105	3.87	3.34	14.83	12.8
$Bp_1m_1F_e\,S_2$	1.79	0.051	3.22	0.092	3.73	0.092	18.41	4.94	25.1	6.74
$Bp_1m_1F_t\,S_2$	1.79	0.051	3.22	0.092	3.73	0.107	5.81	5.03	14.83	12.83
$Bp_1m_2F_e\,S_2$	2.09	0.051	3.77	0.092	4.36	0.108	18.41	4.9	25.1	6.74
$Bp_1m_2F_t\,S_2$	2.09	0.051	3.77	0.092	4.36	0.108	5.81	5.05	14.83	12.8
$Bp_2m_1F_e\,S_2$	1.79	0.051	3.22	0.092	3.8	0.108	18.4	1.01	30.75	8.26
$Bp_2m_1F_t\,S_2$	1.79	0.051	3.22	0.092	3.8	0.108	5.81	5.02	18.16	15.7
$Bp_2m_2F_e\,S_2$	2.09	0.051	3.77	0.092	4.42	0.108	18.4	4.9	30.75	8.25
$Bp_2m_2F_t\,S_2$	2.09	0.051	3.77	0.092	4.42	0.108	5.81	5.01	18.16	15.67

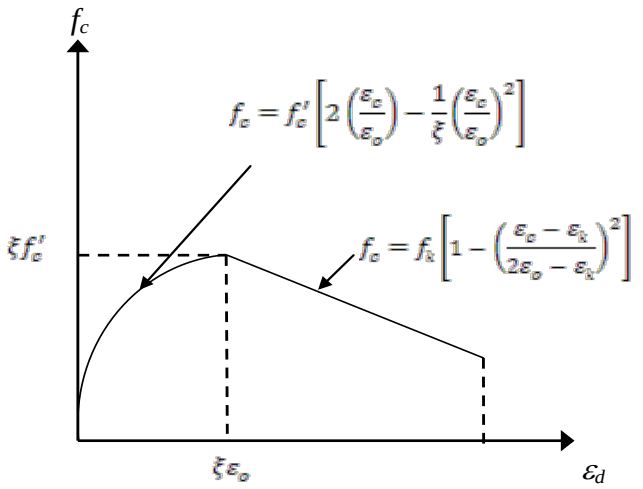

Figure 7: Stress- strain curve for softened concrete

Equilibrium Equations

The in-plane equilibrium equations for the rectangular element can be expressed as

$$f_c cos^2\alpha + \frac{A_{S/GFRP}}{a_o\, t_w} f_{s/GFRP} = 0 \tag{25}$$

$$f_c sin^2\alpha + \frac{A_{S/GFRP-t}}{s_v\, t_w} f_{s/GFRP-t} = 0 \tag{26}$$

$$-f_c sin\alpha\, cos\alpha = \tau \tag{27}$$

where $A_{S/GFRP}$ = total cross sectional area of the longitudinal reinforcements; $A_{S/GFRP\text{-}t}$ = cross sectional area of the one two legged stirrups; a_o = Perimeter of the centerline of the shear flow area; s_v is the center-to-center spacing of the stirrups; f_C = Compressive strength of concrete struts; f_r = tensile strength of concrete which is assumed to zero; α is the angle of inclination of the concrete struts with respect to longitudinal axis.

Based on the equilibrium equation, the torque T is written as,

$$T = 2A_o \tau\, t_w \tag{28}$$

Based on the compatibility equation, the in-plane deformation the rectangular element should satisfy the following three compatibility equations,

$$\varepsilon_{s/GFRP} + \varepsilon_{st/GFRP-t} = \varepsilon_c + \varepsilon_r \quad (29)$$

$$tan^2\alpha = \frac{\varepsilon_{s/GFRP} - \varepsilon_c}{\varepsilon_{st/GFRP-t} - \varepsilon_c} \quad (30)$$

$$\gamma = 2\left(\varepsilon_{st/GFRP-t} - \varepsilon_c\right)tan\alpha \quad (31)$$

where, $\varepsilon_{s/GFRP}$ ≡ strain in longitudinal steel/GFRP reinforcements; $\varepsilon_{s/GFRP-t}$ ≡ strain in transverse steel/GFRP reinforcements (stirrups); ε_c ≡ compressive strain in concrete struts; ε_t ≡ tensile strain in concrete struts; According to thin walled tube theory, the relationship between the shear strain γ and the rate of twist θ can be written as follows:

$$\theta = \frac{a_o}{2A_o}\gamma \quad (32)$$

when the member is subjected to torsion, twisting also produces warping in the wall of the member, which in turn, causes bending in the concrete struts. This relationship is described by

$$\emptyset = \theta sin2\alpha \quad (33)$$

where $\emptyset$ = curvature of the concrete struts. Hence the thickness t_w can be written in terms of $\emptyset$ and the maximum strain at the outer surface of the wall as follows:

$$-\frac{\varepsilon_{su}}{\emptyset} = t_w \quad (34)$$

The above equation is valid assuming the strain distribution through the thickness is linear. ε_{su} extreme fibre strain of the section which is taken as 0.0035. The average strain ε_{avg} defined as the strain corresponding to the place at which the stress resultant is located is assumed to be

$$\frac{\varepsilon_{su}}{2} = \varepsilon_{avg} \quad (35)$$

Combining equations (27) & (28)

$$T = -f_c A_o t_w sin2\alpha \quad (36)$$

Combining equations (33) & (34)

$$-\frac{\varepsilon_{su}}{sin2\alpha \times t_w} = \theta \quad (37)$$

Substituting in equation (37), yields

$$\varepsilon_{su} = \frac{p_o t_w}{2A_o}\gamma sin2\alpha \quad (38)$$

Using equations (30) and (31)

$$\gamma = 2(\varepsilon_{s/GFRP} - \varepsilon_c)cot\alpha \tag{39}$$

Substituting (39) in (38)

$$\varepsilon_{su} = \frac{2t_w p_o}{A_o}(\varepsilon_{s/GFRP} - \varepsilon_{avg})cos_{\alpha}^2 \tag{40}$$

Using Equation (25) and (35)

$$\varepsilon_{s/GFRP} = \varepsilon_{avg} + \frac{A_o f_{avg}}{A_{s/GFRP \times f_{s/GFRP}}}\varepsilon_{avg} \tag{41}$$

Using Equation (31) and (38) yields,

$$\varepsilon_{su} = -\frac{2t_w p_o}{A_o}(\varepsilon_{s/GFRP-t} - \varepsilon_c)sin_{\alpha}^2 \tag{42}$$

Using Equation (26) and (35) yields

$$\varepsilon_{su} = \varepsilon_c + \frac{A_o f_{avg} S}{p_o A_{s/GFRP-t \times f_{s/GFRP-t}}}\varepsilon_c \tag{43}$$

Constitutive Laws of Concrete Struts and Steel

Let the uni-axial stress-strain curve of the concrete struts be expressed by a parabolic curve

$$f = -\beta f_{cy}\left[2\frac{\varepsilon}{\varepsilon_c} - \left\{\frac{\varepsilon}{\varepsilon_c}\right\}^2\right] \tag{44}$$

where ε_c= -0.002; f_{cy}= cylindrical strength of concrete; β factor representing the softening parameter proposed by Vecchico and Collins (1986) is used in this study, which takes the form as

$$\beta = \frac{1}{0.8+170\varepsilon_t} \leq 1 \tag{45}$$

where ε_t= principal tensile strain of the concrete struts. Notice the above equation may not be accurate when $f_{cy} > 35\ MPa$. The concept of stress block still applies for the concrete struts. Therefore the average stress of the concrete struts is given by

$$f_{avg} = -k1\beta f_{cy} \tag{46}$$

where the nondimensional coefficient k_1 is defined as the ratio of the average

stress to the peak stress $-\beta f_{cy}$.

$$k1 = \frac{\varepsilon_{su}}{\varepsilon_c}\left(1 - \frac{\varepsilon_{su}}{3\varepsilon_c}\right) \quad (47)$$

Finally the resultant per unit width C of the softened compression stress block has magnitude $= k1\beta f_{cy} t_w$, and its position is theoretically located at a distance of $k2t_w$ from the extreme fibre. The value of k_2 is in the range of 0.4 to 0.5 but based on Hsu, the assumption of k_2 = 0.5 will simplify the model and have slight effect on the accuracy. The constitute law of steel is assumed to be elastic-perfectly plastic. Elastic modulus for both the longitudinal and transverse steel is denoted by E_s, yield strength by f_L, f_t respectively, and yield strain by ε_L, ε_t respectively.

Geometry Equations

$$A_o = A_c \frac{p_c}{2} t_w + \xi \quad (48)$$

$$p_o = p_c - 4\xi t_w \quad (49)$$

where A_c and $p_c$are the area and perimeter of the cross section respectively. The value of ξ=1 for rectangular sections it is basically geometry dependent. Assuming$\varepsilon_{su} = -0.0035$; $\frac{\varepsilon_{su}}{2} = \varepsilon_{avg}$; Also assuming the initial wall thickness $t_w = 0.75\frac{A_c}{p_c}$ and initial softening coefficient $\beta = 0.5$. The average stress of the concrete struts is given by $f_{st} = -k1\beta f_{cy}$; where k_1= 35/48.

4 Results and Discussion

The results of the theoretical analysis based on the space truss analogy and softened truss model are presented in the form of T-θ curves (Figures 8 – 15) as follows:

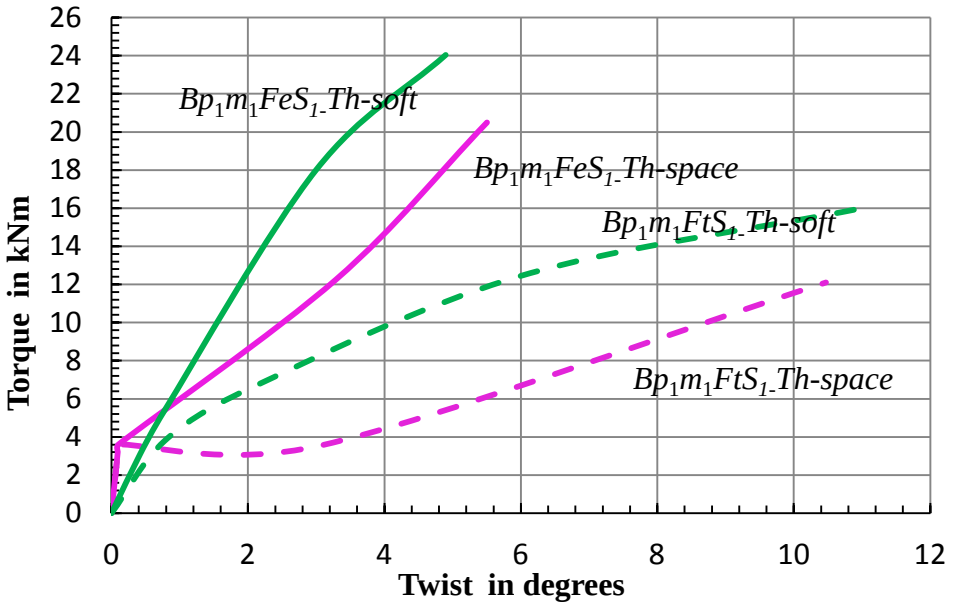

Figure 8: Torque verses twist for $Bp_1m_1F_e\ S_1$ and $Bp_1m_1F_t\ S_1$

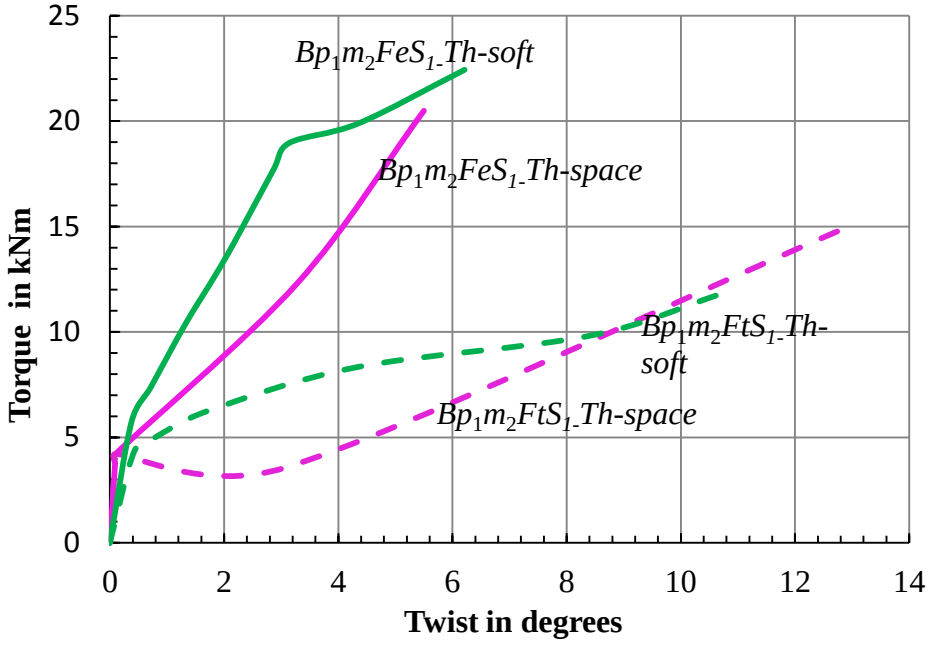

Figure 9: Torque verses twist for $Bp_1m_2F_e\ S_1$ and $Bp_1m_2F_t\ S_1$

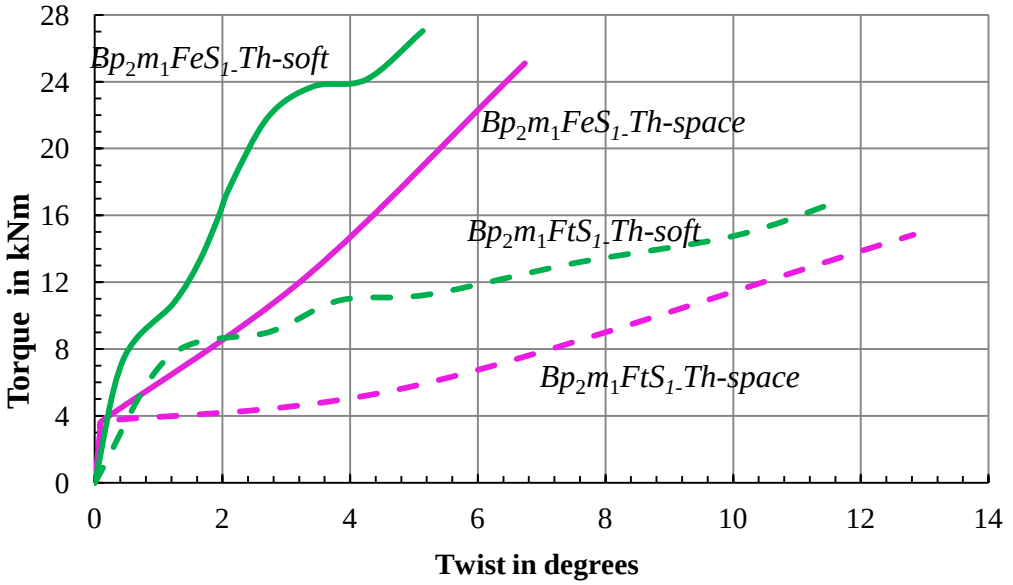

Figure 10: Torque verses twist for $Bp_2m_1F_e\ S_1$ and $Bp_2m_1F_t\ S_1$

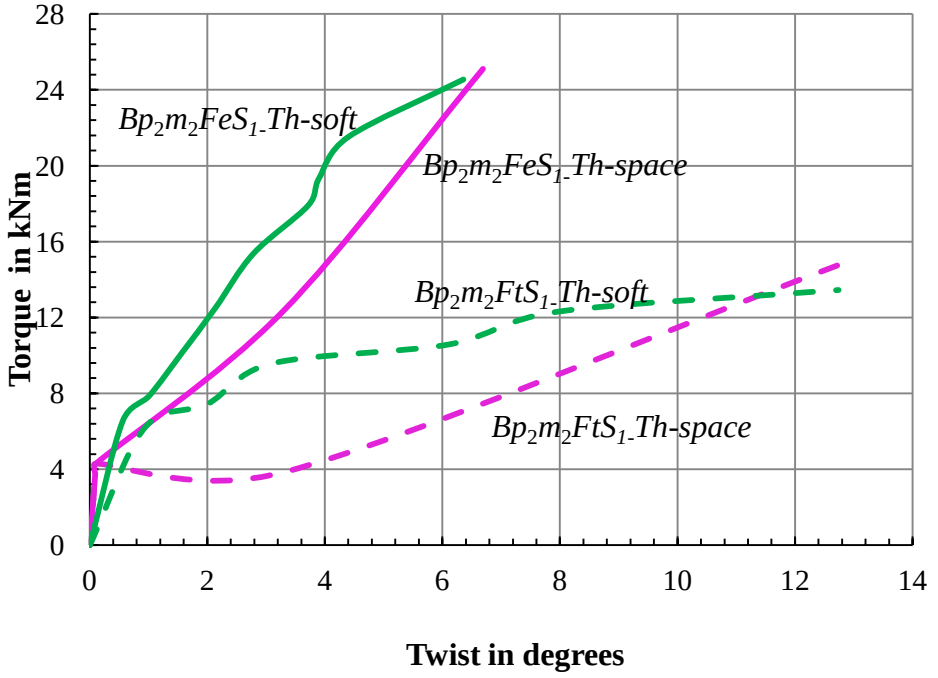

Figure 11: Torque verses Twist for $Bp_2m_2F_e\ S_1$ and $Bp_2m_2F_t\ S_1$

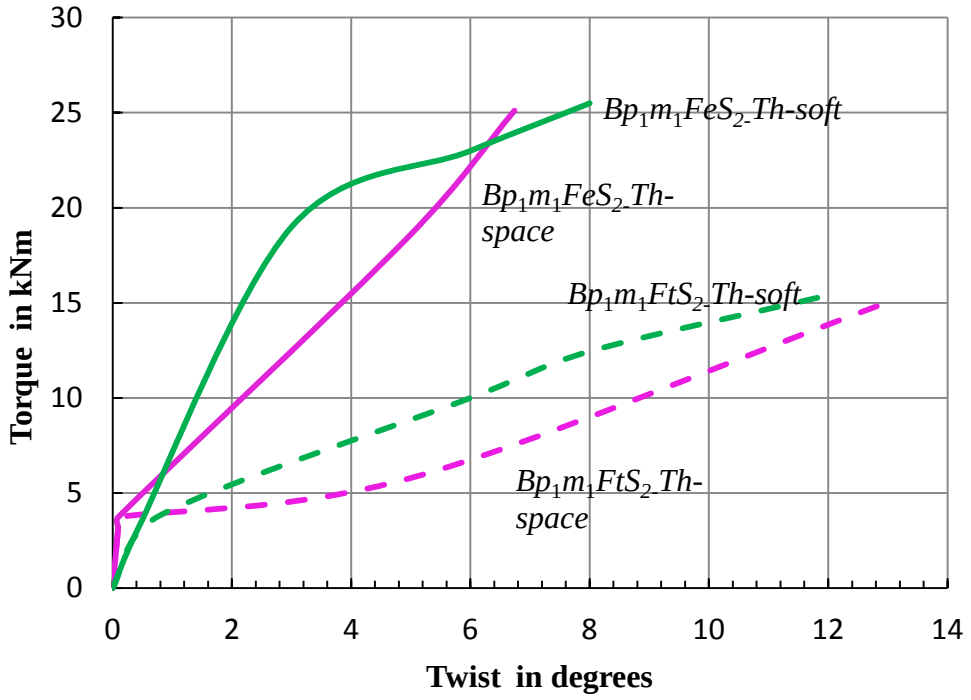

Figure 12: Torque verses Twist for $Bp_1m_1F_e\ S_2$ and $Bp_1m_1F_t\ S_2$

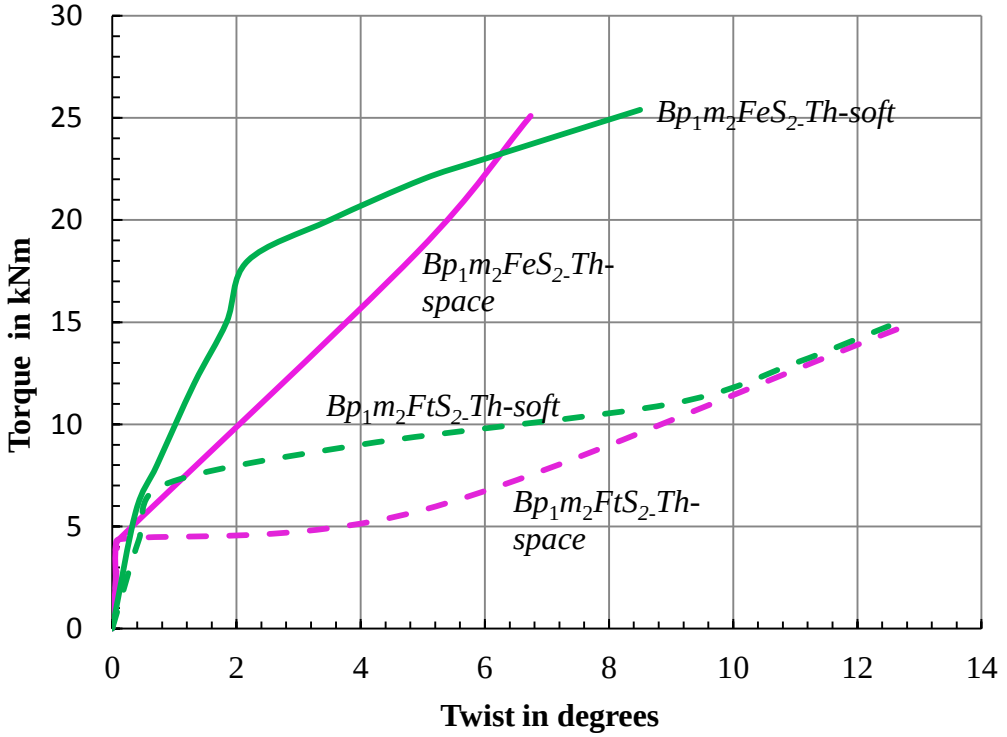

Figure 13: Torque verses Twist for $Bp_1m_2F_e\ S_2$ and $Bp_1m_2F_t\ S_2$

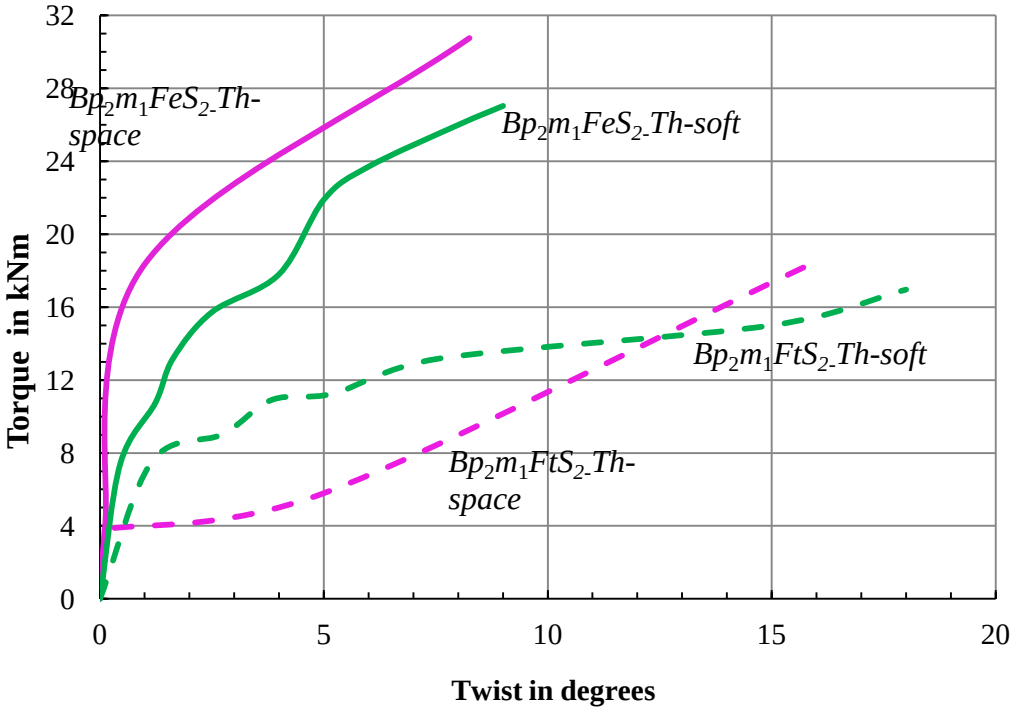

Figure 14: Torque verses Twist for $Bp_2m_1F_e\ S_2$ and $Bp_2m_1F_t\ S_2$

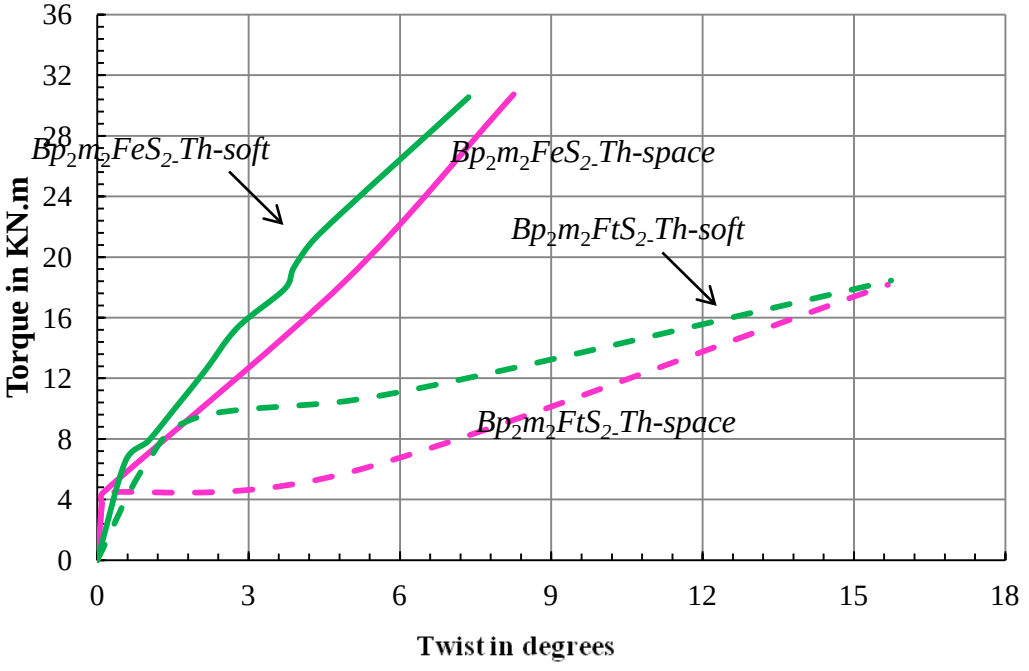

Figure 15: Torque verses Twist for $Bp_2m_2F_e\ S_2$ and $Bp_2m_2F_t\ S_2$

The results of this study are summarized as follows.

- The existing theoretical torque-twist relationship based on space truss analogy and softening truss model for various parametric beams under pure torque condition is utilized for GFRP reinforced concrete beams. The results in the form of torque verses twist diagrams are shown in figures 8 - 15 and the results are compared with the steel reinforced beams.
- The predicted variations of angle of twist with the applied torque for all steel reinforced beams show that ductility of the beams in the post cracking stages is significantly increased for lower percentage of steel (0.56%). But theses variations much higher for GFRP reinforced beams due to higher tensile strains despite the brittle nature of reinforcements.
- The ultimate values of angle of twist and applied torque for parametric conditions are derived and compared with the experimental values. Softening truss model predicts more accurately for GFRP reinforced beams and the variations are less than 10%.
- Torsional strength and angle of twist increases with the increase in increase of grade of concrete and percentage of longitudinal and transverse reinforcements. But GFRP reinforced concrete beams show higher angle of twist than the conventional reinforcements (Figures 8 - 15). This fact is primarily due to higher tensile strain values for GFRP reinforcements than the steel reinforcements.

5 Conclusions

The predicted variations of angle of twist with the applied torque for steel/GFRP reinforced beams show that a closer and almost similar trend when compared to the experimental trend. Therefore the existing theories using space truss analogy and softening truss model are more reliable to predict the torsional behaviour. It is also noted that the replacing main and transverse steel

reinforcements by an equal percentage of GFRP reinforcements, reduced their torsional capacities. The ultimate values of torsional strength of beams have greater influence on the spacing of stirrups. The minimum spacing of stirrups are arrived based on the Indian Standards. An examination of the curves reveals that the slope of the curves at the initial stages of loading is mild for GFRP reinforced beams whereas for conventional beams it is steeper. This is primarily due lower elastic modulus than conventional steel reinforcements.

References

[1] ACI 440R-96, State of the Art Report on Fiber Reinforced Plastic Reinforcement for Concrete Structures, *ACI Committee 440*, American Concrete Institute (ACI), Detroit, 1996.

[2] ACI 400-3R-04, Guide Test Methods for Fiber Reinforced Polymers (FRP) for Reinforcing or Strengthening Concrete Structures, *ACI Committee 440*, American Concrete Institute (ACI), 2004.

[3] ACI Committee 440.XR, Report on Fiber Reinforced Polymer (FRP) Reinforcement for Concrete Structures, American Concrete Institute (ACI), 2007.

[4] ASTM-D 3916-84**,** Standard Test Methods for Tensile properties of Pultruded Glass-Fibre Reinforced Plastic Rod.

[5] Asghar Bhatti, M. and Anan Almughrabi, Refined Model to Estimate Torsional Strength of Reinforced Concrete Beams, *ACI Journal of Structural Engineering*, **93**, (1996), 614-622.

[6] Bank C. Lawrence, Moshe Puterman and Ammon Katz, The Effect of Material Degradation on Bond properties of Fiber Reinforced Plastic Reinforcing Bars in Concrete, *ACI Materials Journal*, **95**(3), (1998), 232-243.

[7] B. Benmokrane, O. Chaallal and R. Masmoudi, Flexural Response of Concrete Beams Reinforced with FRP Reinforcing Bars, *ACI Materials Journal*, **91**(2), (1995), 46–55.

[8] CAN/CSA-S806, *Design and Construction of Building Components with Fibre Reinforced Polymers, Canadian Standards Association*, Mississauga, Ontario, Canada, 2002.

[9] CEB-FIP, *FRP Reinforcement in RC Structures*, Committee Euro-International du Beton, Thomas Telford Services Ltd, London, 2007.

[10] Chyan-Hwan Jeng, Simple Rational Formulas for Cracking Torque and Twist of Reinforced Concrete Members, *ACI Structural Journal*, **107**(2), (2010), 180-197.

[11] M.P. Collins, *Torque-Twist Characteristics of Reinforced Concrete Beams Inelasticity and Non-linearity in Structural Concrete Study*, No.8, University of Waterloo press, Waterloo, Canada, 211-232, (1973).

[12] H.J. Cowan, Elastic Theory for Torsional Strength of Rectangular Reinforced Concrete Beams, *Magazine of Concrete Research London*, **2**(4), (1950), 3-8.

[13] Craig R. Michaluk, Sami H. Rizkalla, Gamil Tadros and Brahim Benmokrane, Flexural Behavior of One-way Concrete Slabs Reinforced by Fibre Reinforced Plastic Reinforcements, *ACI Structural Journal*, **95**(3), (1998), 353-364.

[14] A. Deiveegan and G. Kumaran, A Study of Combined Bending and Axial Load on Concrete Columns Reinforced with Non-Metallic Reinforcements, *Central European Journal of Engineering*, Warsaw, Poland, **56**(4), (2011), 562-572.

[15] S.S. Faza and H.V.S. GangaRao, Bending and Bond Behaviour of Concrete Beams Reinforced with Fibre Reinforced Plastic Rebars, *WVDOH-RP-83 Phase 1 Report*, West Virginia University, Morgantown, (1992), 128-173.

[16] H.G. Filippou Kwak and C. Filip, *Finite Elements Analysis of Reinforced Structures under Monotonic Loads*, A report on research conducted in Department of Civil Engineering, University of California, Berkeley, 1990.

[17] T.T.C. Hsu, Ultimate Torque of Reinforced Rectangular Beams, *ASCE Journal Structural Division*, **94**, (Feb., 1968), 485–510.

[18] T.T.C. Hsu and YL Mo, Softening of Concrete in Torsional Members-Design Recommendations, *Journal of the American Concrete Proceedings*, **82**(4), (1985), 443–452.

[19] T.T.C. Hsu, Softened Truss Model Theory for Shear and Torsion, *ACI Structural Journal*, **85**(6), (1988), 624-635.

[20] IS: 516, Code of Practice-Methods of Test for Strength of Concrete, *Bureau of Indian standards*, New Delhi, India, 1959.

[21] IS: 10262, Guide Lines for Concrete Mix Design, *Bureau of Indian Standards*, New Delhi, India, 1982.

[22] IS: 456, Code of Practice for Plain & Reinforced Concrete, *Bureau of Indian Standards*, Indian Standards Institution, New Delhi, India, 2000.

[23] Khaldoun N. Rahal and M.P. Collins, Simple Model for Predicting Torsional Strength of Reinforced and Prestressed Concrete Sections, *Journal of American Concrete Inst Proceedings*, **93**(6), (1996), 658–666.

[24] Liang-Jenq Leu and Yu Shu Lee, Torsion Design Charts for Reinforced Concrete Rectangular Members, *Journal of Structural Engineering*, **126**(2), (2000), 210-218.

[25] F.A. Bernardo Luis and Sergio M.R. Lopes, Behaviour of Concrete Beams under Torsion: NSC Plain and Hollow Beams, *Journal of Material and Structures*, **41**, (2008), 1143-1167.

[26] A. Machida, *State-of-the-Art Report on Continuous Fiber Reinforcing Materials, Society of Civil Engineers (JSCE)*, Tokyo, Japan, 1993.

[27] J.G. MacGregor and M.G. Ghoneim, Design for Torsion, *Journal of the American Concrete*, **92**(2), (1995), 211–218.

[28] A. Nanni, Flexural Behaviour and Design of RC Members using FRP Reinforcement, *Journal of the Structural Engineering (ASCE),* **119**(11), (1993), 3344–3359.

[29] E. Rausch, *Design of Reinforced Concrete in Torsion*, PhD Thesis, Technische Hochshule, Berlin, 1929.

[30] J. Saravanan and G. Kumaran, Joint Shear Strength of FRP Reinforced Concrete Beam-Column Joints, *Central European Journal of Engineering,* Warsaw, Poland, **1**(1), (March, 2011), 89-102.

[31] R. Sivagamasundari, *Experimental and Analytical Investigations on the Behaviour of Concrete Slabs Reinforced with Fibre Based Rods as Flexural reinforcements,* Ph.D Thesis, Department of Civil & Structural Engineering, Annamalai University, Annamalai Nagar, India, 2008.

[32] S. Unnikrishna Pillai and Devdas Menon, *Reinforced Concrete Design,* Tata Mc Graw-Hill Publishing Company Limited, New Delhi, India, 2003.